Diabetologia (2018) 61:1384–1396
https://doi.org/10.1007/s00125-018-4593-3

ARTICLE

Targeted delivery of antigen to intestinal dendritic cells induces oral tolerance and prevents autoimmune diabetes in NOD mice

Yulin Chen[1] · Jie Wu[2] · Jiajia Wang[1] · Wenjing Zhang[1] · Bohui Xu[1] · Xiaojun Xu[3] · Li Zong[1]

Received: 12 November 2017 / Accepted: 19 February 2018 / Published online: 15 March 2018

Abstract

Aims/hypothesis The intestinal immune system is an ideal target to induce immune tolerance physiologically. However, the efficiency of oral protein antigen delivery is limited by degradation of the antigen in the gastrointestinal tract and poor uptake by antigen-presenting cells. Gut dendritic cells (DCs) are professional antigen-presenting cells that are prone to inducing antigen-specific immune tolerance. In this study, we delivered the antigen heat shock protein 65-6×P277 (H6P) directly to the gut DCs of NOD mice through oral vaccination with H6P-loaded targeting nanoparticles (NPs), and investigated the ability of this antigen to induce immune tolerance to prevent autoimmune diabetes in NOD mice.

Methods A targeting NP delivery system was developed to encapsulate H6P, and the ability of this system to protect and facilitate H6P delivery to gut DCs was assessed. NOD mice were immunised with H6P-loaded targeting NPs orally once a week for 7 weeks and the onset of diabetes was assessed by monitoring blood glucose levels.

Results H6P-loaded targeting NPs protected the encapsulated H6P from degradation in the gastrointestinal tract environment and significantly increased the uptake of H6P by DCs in the gut Peyer's patches (4.1 times higher uptake compared with the control H6P solution group). Oral vaccination with H6P-loaded targeting NPs induced antigen-specific T cell tolerance and prevented diabetes in 100% of NOD mice. Immune deviation (T helper [Th]1 to Th2) and $CD4^+CD25^+FOXP3^+$ regulatory T cells were found to participate in the induction of immune tolerance.

Conclusions/interpretation In this study, we successfully induced antigen-specific T cell tolerance and prevented the onset of diabetes in NOD mice. To our knowledge, this is the first attempt at delivering antigen to gut DCs using targeting NPs to induce T cell tolerance.

Keywords Autoimmune diabetes · Dendritic cells · Nanoparticles · NOD mice · Oral tolerance · Oral vaccination

Electronic supplementary material The online version of this article (https://doi.org/10.1007/s00125-018-4593-3) contains peer-reviewed but unedited supplementary material, which is available to authorised users.

✉ Xiaojun Xu
xiaojunxu2000@163.com

✉ Li Zong
zongCPU@126.com

[1] Department of Pharmaceutics, China Pharmaceutical University, 24 TongJiaXiang, Nanjing 210009, People's Republic of China

[2] Minigene Pharmacy Laboratory, China Pharmaceutical University, Nanjing, People's Republic of China

[3] State Key Laboratory of Natural Medicines, China Pharmaceutical University, 24 TongJiaXiang, Nanjing 210009, People's Republic of China

Abbreviations

CFSE	Carboxyfluorescein succinimidyl ester
CLSM	Confocal laser scanning microscopy
ConA	Concanavalin A
CS	Chitosan
DC	Dendritic cell
FITC-H6P	FITC-labelled heat shock protein 65-6×P277
FRET	Fluorescence resonance energy transfer
H6P	Heat shock protein 65-6×P277
H6P/RMCS	Heat shock protein 65-6×P277-loaded RGD- and mannose-modified chitosan
HSP	Heat shock protein
i.g.	Intra-gastric
MCS	Mannose-modified chitosan

Research in context

What is already known about this subject?

- Previous preclinical and clinical data indicate the potential for orally administered autoantigens to induce immune tolerance in type 1 diabetes
- Gut dendritic cells tend to induce immune tolerance

What is the key question?

- Do targeting nanoparticles facilitate antigen uptake by gut dendritic cells and prevent diabetes in NOD mice?

What are the new findings?

- Targeting nanoparticles protected the encapsulated antigen from degradation in the gastrointestinal tract environment and facilitated uptake of the antigen by gut dendritic cells
- Oral vaccination with heat shock protein 65-6×P277 (H6P)-loaded targeting nanoparticles efficiently induced antigen-specific T cell tolerance and prevented diabetes in NOD mice

How might this impact on clinical practice in the foreseeable future?

- The use of antigen-loaded targeting nanoparticles may reduce the dosage and dosing frequency required for oral antigen-specific therapy and favour the induction of immune tolerance in clinical practice

NP	Nanoparticle
RCS	RGD-modified chitosan
RGD	Arginylglycylaspartic acid
RMCS	RGD- and mannose-modified chitosan
SGF	Simulated gastric fluid
SIF	Simulated intestinal fluid
Th	T helper
Treg	Regulatory T cell

Introduction

The exact cause of type 1 diabetes remains elusive. Usually, it is considered to be a chronic autoimmune disease in which pancreatic beta cells are destroyed or damaged by the body's own immune system, causing insulin deficiency [1]. In individuals with type 1 diabetes, glycaemic control is achieved by daily injections or continuous s.c. infusion of insulin. However, there is currently no cure for the condition. Attempts to prevent or cure type 1 diabetes using immunotherapy that are being investigated in clinical trials include non-antigen-specific therapy (e.g. T/B cell depleting strategies, anti-inflammatory strategies or cell therapy strategies) and antigen-specific therapy (e.g. oral/nasal insulin, alum-formulated GAD65, proinsulin peptides or DiaPep277) [2, 3].

Antigen-specific therapy has been considered the 'Holy Grail' of immunotherapy for type 1 diabetes because it targets only beta cell reactive T cells without impairing beneficial immune responses. Peptide P277 is a 24 amino acid fragment of heat shock protein (HSP)60/65 that has been found to be an autoantigen for diabetogenic T cell clones in NOD mice and individuals with type 1 diabetes [4, 5]. In previous work, we successfully constructed a heat shock protein 65-6×P277 (H6P) vaccine, based on autoantigen P277, against autoimmune diabetes in NOD mice [6]. For vaccination, autoantigens can be delivered via different routes, including intraperitoneal, intravenous, oral and intranasal administration [7]. The administration route of a vaccine plays an important role in inducing an antigen-specific immune response and influences clinical efficacy [8]. It is commonly considered that oral administration of antigens is more efficient for tolerance induction, because the intestinal immune system has a predisposition to induce tolerance [9] and its immunosuppressive environment can affect the lymphocytes [10–12]. Dendritic cells (DCs) are professional antigen-presenting cells with the capacity to instigate either inflammatory or anti-inflammatory adaptive immunity. The direction of the response is influenced by DC phenotype: either an activated phenotype or, conversely, a tolerogenic phenotype [13]. It has been reported that DCs from gut Peyer's patches tend to induce differentiation of T helper (Th)2 cells and secretion of anti-inflammatory cytokines [14–16] and are prone to inducing regulatory T cells (Tregs), which migrate and suppress damaging immune responses and secrete antigen non-specific cytokines such as TGF-β, contributing to bystander suppression [17].

In this study, we attempted to induce immune tolerance in NOD mice through the oral delivery of H6P to the DCs in gut Peyer's patches. However, it is difficult for oral antigens to

reach gut DCs because of the poor stability of antigens in the gastrointestinal tract and the absorption barriers presented by the intestinal mucus layer and the epithelial cell layer [18], which leads to low treatment efficiency. M cells are specialised epithelial cells that are mainly located in the follicle-associated epithelium of Peyer's patches [19] and have high transcytotic capabilities to transport a broad range of materials from the intestinal lumen to the DCs in Peyer's patches [20]. The specific location and function of M cells make them an attractive target for oral vaccine delivery to DCs. Thus, we developed a delivery system based on the M cell targeting peptide arginylglycylaspartic acid (RGD) [21] and DC-targeting ligand mannose [22]-modified chitosan (CS) nanoparticles (NPs), to protect and facilitate H6P antigen delivery to gut DCs, hoping to improve treatment efficiency. In this study, we aimed to investigate whether oral H6P-loaded targeting NPs could deliver H6P to DCs in gut Peyer's patches and prevent autoimmune diabetes through the induction of T cell tolerance.

Methods

Mice Four-week-old female NOD/LtJ mice were purchased from Beijing HFK Bioscience (Beijing, China). Six- to 8-week-old female BALB/c mice were obtained from Qinglongshan Laboratory Animal Center (Nanjing, China). Mice were housed in a pathogen-free facility with temperature (23 ± 1°C) and light (12 h light/dark cycle) control, and had free access to water and standard mouse chow. Animal care and all experiments in this study were conducted in accordance with the Provision and General Recommendation of Chinese Experimental Animals Administration Legislation and approved by the China Pharmaceutical University Institutional Animal Care and Use Committee. The investigators were not blinded to the experimental groups, unless otherwise noted.

Reagents Full details of the reagents used in this study are provided in the electronic supplementary material (ESM) Methods.

Synthesis of RGD- and mannose-modified chitosan Mannose-modified chitosan (MCS) was synthesised as previously described [23]. RGD-modified chitosan (RCS) or RGD- and mannose-modified chitosan (RMCS) were synthesised by using a crosslinking reagent, *N*-succinimidyl-3-(2-pyridyldithio)-propionate, to conjugate RGD to the amino groups of CS or MCS [24]. Details are provided in the ESM Methods.

Preparation and characterisation of NPs NPs were prepared by electrostatic self-assembly of oppositely charged polysaccharides at room temperature. Details are provided in the ESM Methods. The particle size, zeta potential value, association efficiency and drug loading of NPs were characterised, and details are provided in the ESM Methods.

In vitro release of H6P from H6P-loaded RMCS NPs The H6P release profile of H6P-loaded RMCS (H6P/RMCS) NPs was separately evaluated in 0.1 mol/l HCl (pH 1.0) and PBS (pH 6.8). Details are provided in the ESM Methods.

Stability of H6P/RMCS NPs The stability of H6P/RMCS NPs in simulated gastric fluid (SGF; containing pepsin, pH 1.2, USP 38) and simulated intestinal fluid (SIF; containing pancreatin, pH 6.8, USP 38) was tested by measuring changes in particle size and fluorescence resonance energy transfer (FRET) efficiency after a 6 h incubation. Further details are provided in the ESM Methods.

Structural integrity of the H6P antigen The structural integrity of H6P after encapsulation in RMCS NPs was assessed by SDS-PAGE as previously described [25], with some modifications. The protective effects of RMCS NPs on H6P against degradation in SGF (containing pepsin, pH 1.2, USP 38) and SIF (containing pancreatin, pH 6.8, USP 38) were also assessed in vitro using SDS-PAGE. Details are provided in the ESM Methods.

Evaluation of FITC-labelled H6P delivery efficiency to Peyer's patches The delivery efficiencies of FITC-labelled H6P (FITC-H6P) loaded in CS NPs or RCS NPs were evaluated using confocal laser scanning microscopy (CLSM) as previously described [26], with some modifications. Details are provided in the ESM Methods.

Evaluation of FITC-H6P uptake by DCs in Peyer's patches The uptake of FITC-H6P loaded in CS NPs, MCS NPs or RMCS NPs by DCs in Peyer's patches was evaluated using flow cytometry. FITC-H6P solution was used as a control. Details are provided in the ESM Methods.

Vaccination Four-week-old female NOD mice were randomly divided into four groups (ten mice per group). Mice in three groups were given an oral gavage of H6P solution (H6P intra-gastric [i.g].), blank RMCS NPs (RMCS NPs i.g.) or H6P/RMCS NPs (H6P/RMCS NPs i.g.), respectively. Mice in the fourth group were given an s.c. injection of H6P solution (H6P s.c.). Each mouse was immunised with a dose of 100 μg H6P at 4, 5, 6, 7, 8, 9 and 10 weeks of age.

Analytical measurements and histological analysis The blood glucose levels of NOD mice were monitored from 7 to 23 weeks of age. Mice were diagnosed as having diabetes once the blood glucose level was higher than 11 mmol/l for two consecutive days. Serum insulin levels were determined

using a commercial ELISA kit. Insulitis and insulin immunohistochemistry were analysed as previously reported [27, 28]. Further details are provided in the ESM Methods.

Determination of H6P-specific antibodies The presence of H6P-specific antibodies was determined using ELISA. Details are provided in the ESM Methods.

Mechanistic studies Four-week-old female NOD mice were randomly divided into three groups (four mice per group) and immunised with RMCS NPs i.g., H6P/RMCS NPs i.g. or H6P s.c. The vaccination process was as described in the 'Vaccination' section above. Four weeks after the last administration, T cell proliferation responses to H6P were assessed using a carboxyfluorescein succinimidyl ester (CFSE)-based method; cytokine secretion after H6P stimulation was determined using commercial ELISA kits; and the presence of Tregs and Th1 cells in pancreatic draining lymph nodes was analysed using flow cytometry. Details are provided in the ESM Methods.

Statistical analyses Data were evaluated using SPSS Statistics version 17 (SPSS, Chicago, IL, USA). Data are expressed as means ± SD. Statistical significance was determined using the independent-samples *t* test. The log rank test was used to compare diabetes incidence curves. $p < 0.05$ indicated statistical significance. No inclusion or exclusion criteria were applied.

Results

Synthesis and characterisation of RMCS The synthetic scheme for RMCS is shown in ESM Fig. 1. The structures of MCS, RCS and RMCS were confirmed using ^{1}H NMR (Fig. 1a). As shown in Fig. 1b, the multiple peaks within 3.5–4.0 ppm (arrow) correspond to the protons of mannose overlapping with the protons of CS, which confirmed the conjugation of mannose with CS [23]. In Fig. 1c, the conjugation of RGD with CS was confirmed by the appearance of characteristic peaks at 7.2–7.4 ppm (arrowhead), which were assigned to the protons of benzene ring in phenylalanine of the RGD peptide [24]. The characteristic peaks at 3.5–4.0 ppm (arrow) and 7.2–7.4 ppm (arrowhead) in Fig. 1d demonstrated that both RGD and mannose were conjugated with CS. The degree of substitution of mannose in MCS was 7.1%. The

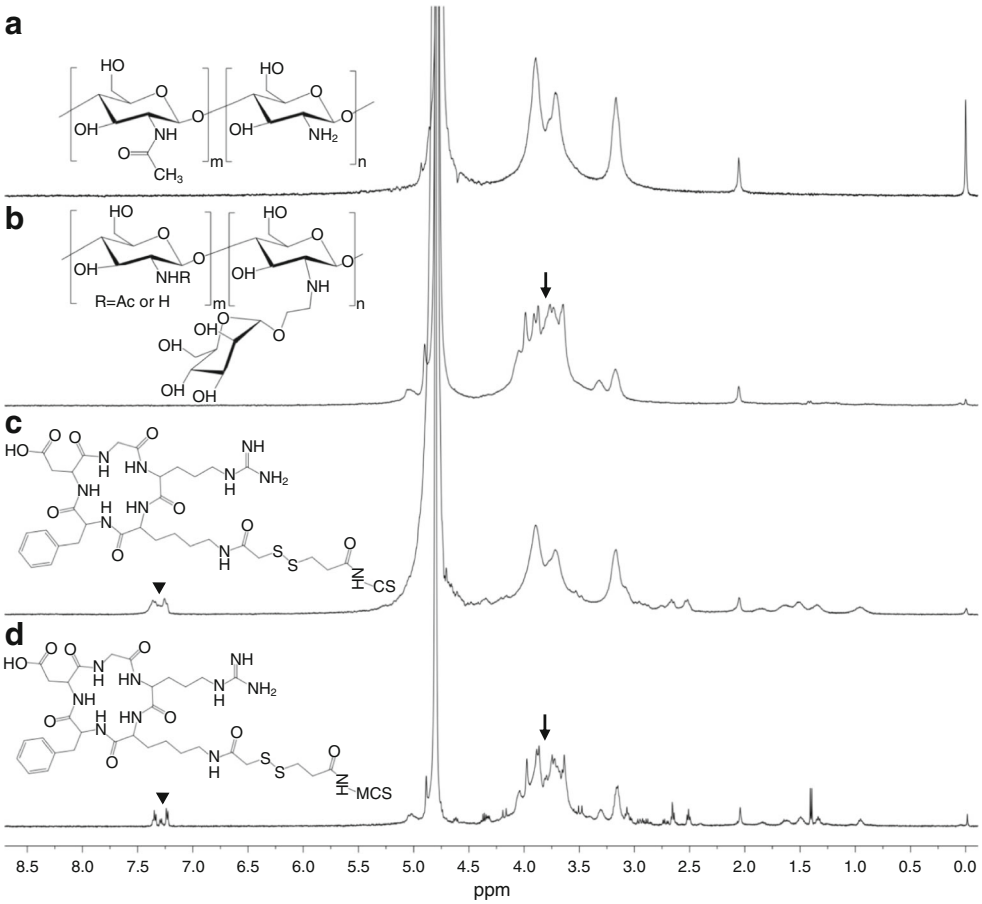

Fig. 1 ^{1}H NMR spectra of (**a**) CS, (**b**) MCS, (**c**) RCS and (**d**) RMCS. Representative results are shown from three independent experiments. Arrows indicate the conjugation of mannose and arrowheads indicate the conjugation of RGD

Table 1 Characteristics of RMCS NPs and H6P/RMCS NPs

NP	Size (nm)	Zeta potential (mV)	Association efficiency (%)	Drug loading (%)
RMCS	312.1 ± 5.6	33.5 ± 0.4	–	–
H6P/RMCS	322.5 ± 6.1	34.9 ± 0.5	91.5 ± 2.7	11.2 ± 2.6

Data are means ± SD

n=3

degree of substitution of RGD in RCS and RMCS was 6.0% and 5.6%, respectively.

Preparation and characterisation of H6P/RMCS NPs H6P/RMCS NPs were formulated by intermolecular crosslinking between positively charged RMCS and negatively charged dextran sulphate. H6P was positively charged at pH 3.0 and incorporated into NPs through electrostatic interaction. As neither an organic solvent nor high-energy input is required in the electrostatic self-assembly of an H6P/RMCS NP, this NP is particularly suitable for the delivery of biological macromolecular drugs. The characteristics of RMCS NPs and H6P/RMCS NPs are listed in Table 1. A transmission electron microscope image of H6P/RMCS NPs is shown in Fig. 2a.

The in vitro release profiles of H6P from H6P/RMCS NPs at pH 1.0 and pH 6.8 are shown in Fig. 2b. The results indicated that less than 4.1% H6P was released from H6P/RMCS NPs at pH 1.0 (simulating the pH of the stomach). At pH 6.8, however, a burst release of H6P from H6P/RMCS NPs was observed within 0.5 h, followed by sustained release.

The stability of H6P/RMCS NPs in SGF or SIF was evaluated by particle size and FRET analysis, respectively. The particle size of H6P/RMCS NPs remained almost unchanged in SGF, but increased to 524.8 ± 10.9 nm within 0.5 h in SIF (Fig. 2c). Although the swelling or aggregation of NPs can be monitored by changes in particle size, any leakage of the encapsulated H6P may not be precisely reflected. FRET analysis can cope with this issue without any pretreatment. Since a FRET signal occurs only when the two probes are in close proximity (<10 nm), any leakage of FITC-H6P reduces FRET efficiency [29]. The fluorescence spectrum of FRET

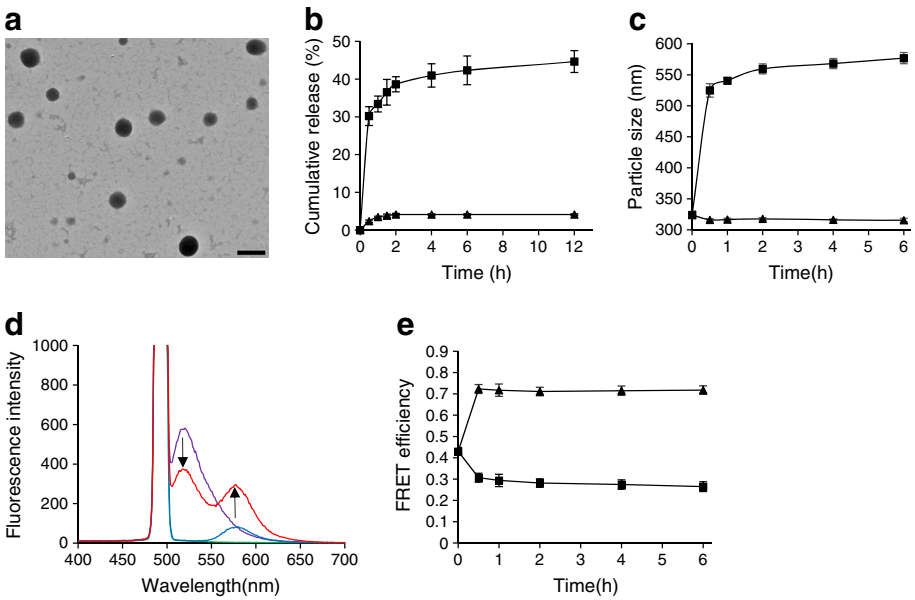

Fig. 2 (**a**) Transmission electron microscope image of H6P/RMCS NPs. Scale bar, 500 nm. (**b**) The in vitro release profiles of H6P from H6P/RMCS NPs at pH 1.0 (triangles) or pH 6.8 (squares). (**c**) Particle size of H6P/RMCS NPs in SGF (triangles) or SIF (squares) at different time points. (**d**) Fluorescence emission spectra of blank RMCS NPs (green line), FITC-RMCS NPs (purple line), rhodamine B isothiocyanate-RMCS NPs (blue line) and FRET RMCS NPs (red line) with excitation at 493 nm. Down arrow indicates the emission intensity of FITC decreased at 518 nm, up arrow indicates the emission intensity of rhodamine B isothiocyanate increased at 580 nm. (**e**) The FRET efficiency of FRET RMCS NPs in SGF (triangles) or SIF (squares) at different time points. Representative results are shown from three independent experiments. Error bars indicate SDs

RMCS NPs is shown in Fig. 2d. The emission intensity of FITC decreased at 518 nm and the emission intensity of rhodamine B isothiocyanate increased at 580 nm, implying energy transfer from the donor to the acceptor. As shown in Fig. 2e, the FRET efficiency of NPs increased in SGF, suggesting the formation of more tightly packed NPs that protected the loaded H6P from degradation. In SIF, the FRET efficiency of NPs decreased obviously within 0.5 h, and then decreased gradually. The results suggest that FITC-H6P started to be released from NPs in SIF.

Structural integrity of H6P The structural integrity of H6P is very important for retaining its activity. Therefore, the impact of the preparation process on the structure of H6P and the protective effects of RMCS NPs on H6P against degradation in SGF or SIF were assessed using SDS-PAGE. As shown in Fig. 3a, the bands of H6P released from H6P/RMCS NPs (lane 3) were similar to those of native H6P (lane 2), indicating that H6P was not degraded during the preparation process.

The first prerequisite for effective oral protein delivery is to protect the protein from the harsh conditions in the gastrointestinal environment. As shown in Fig. 3, native H6P was degraded in SGF (Fig. 3b, lane 3) or SIF (Fig. 3c, lane 3). However, H6P released from H6P/RMCS NPs after pretreatment with SGF (Fig. 3b, lane 4) or SIF (Fig. 3c, lane 4) showed a target H6P band and no degradation bands. The results suggest that H6P/RMCS NPs effectively protect H6P from degradation in SGF or SIF.

RCS NPs increased FITC-H6P delivery efficiency to Peyer's patches The properties of FITC-H6P/CS NPs and FITC-H6P/RCS NPs are listed in ESM Table 1. A CLSM image of a Peyer's patch is shown in Fig. 4a, and the compartments of the Peyer's patch are outlined and labelled. Fig. 4 shows representative CLSM images of a Peyer's patch treated with FITC-H6P/CS NPs (Fig. 4b) or FITC-H6P/RCS NPs (Fig. 4c) and a villus region treated with FITC-H6P/RCS NPs (Fig. 4d). As shown in Fig. 4e, the fluorescence intensity of FITC in the Peyer's patch treated with FITC-H6P/RCS NPs was significantly higher than that following treatment with FITC-H6P/CS NPs ($p < 0.01$). In addition, the distribution of FITC-H6P in the Peyer's patch was obviously higher than that in the villus region after treatment with FITC-H6P/RCS NPs (Fig. 4e). These results suggest that RGD-modified NPs may increase FITC-H6P delivery efficiency to Peyer's patches through M cell-mediated transcytosis. Non-specific absorption in the villus region was present, but the intensity was quite low.

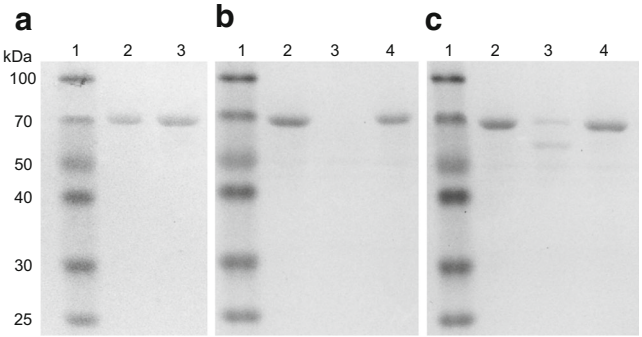

Fig. 3 (**a**) Evaluation of the structural integrity of H6P released from RMCS NPs. Lane 1: marker; lane 2: native H6P; lane 3: H6P released from RMCS NPs. (**b**) Evaluation of the protective effect of RMCS NPs on H6P in SGF. Lane 1: marker; lane 2: native H6P; lane 3: native H6P pretreated with SGF; lane 4: H6P released from RMCS NPs after treatment with SGF. (**c**) Evaluation of the protective effect of RMCS NPs on H6P in SIF. Lane 1: marker; lane 2: native H6P; lane 3: native H6P pretreated with SIF; lane 4: H6P released from RMCS NPs after treatment with SIF. Representative results are shown from three independent experiments

Evaluation of FITC-H6P uptake by DCs in Peyer's patches The properties of FITC-H6P/CS NPs, FITC-H6P/MCS NPs and FITC-H6P/RMCS NPs are shown in ESM Table 1. FITC-H6P uptake by DCs in Peyer's patches (Fig. 5a,b) was analysed based on FITC fluorescence in $CD11c^+$ cells as described previously [30]. In Fig. 5c, $14.1 \pm 1.0\%$ of $CD11c^+$ cells in a Peyer's patch treated with FITC-H6P/MCS NPs were positive for FITC, which was significantly higher than that of FITC-H6P/CS NPs ($p < 0.01$). The enhanced uptake of FITC-H6P by $CD11c^+$ cells might be attributed to the DC-targeting effect of mannose-modified NPs. Moreover, for FITC-H6P/RMCS NPs, $18.5 \pm 1.2\%$ of $CD11c^+$ cells in the Peyer's patch were positive for FITC (4.1 times higher uptake compared with the control H6P solution group). These results indicate that FITC-H6P encapsulated in RMCS NPs was most effectively delivered into $CD11c^+$ cells in the Peyer's patch.

Oral vaccination with H6P/RMCS NPs prevented autoimmune diabetes in NOD mice Prior to the onset of diabetes, 4-week-old NOD mice were treated with H6P i.g., RMCS NPs i.g., H6P/RMCS NPs i.g. or H6P s.c. Mice treated with H6P i.g. or RMCS NPs i.g. started to develop diabetes at 13 weeks of age, and 90% were diabetic at 23 weeks of age (Fig. 6a). In contrast, the diabetes incidence at 23 weeks in the H6P/RMCS NPs i.g. group and the H6P s.c. group was 0% and 40%, respectively; differences between groups were statistically significant (Fig. 6a). At 23 weeks of age, nine mice in the RMCS NPs i.g. group exhibited hyperglycaemia (Fig. 6b), severe insulitis (Fig. 6c,e), loss of beta cells and loss of beta cell function (Fig. 6d,e). By contrast, in the H6P/RMCS NPs i.g. group, no mice showed hyperglycaemia (Fig. 6b) and mice had a predominantly normal islet structure (Fig. 6c,e) and beta cell function (Fig. 6d,e). The results indicate that oral vaccination with H6P/RMCS NPs prevented the onset of autoimmune diabetes in NOD mice.

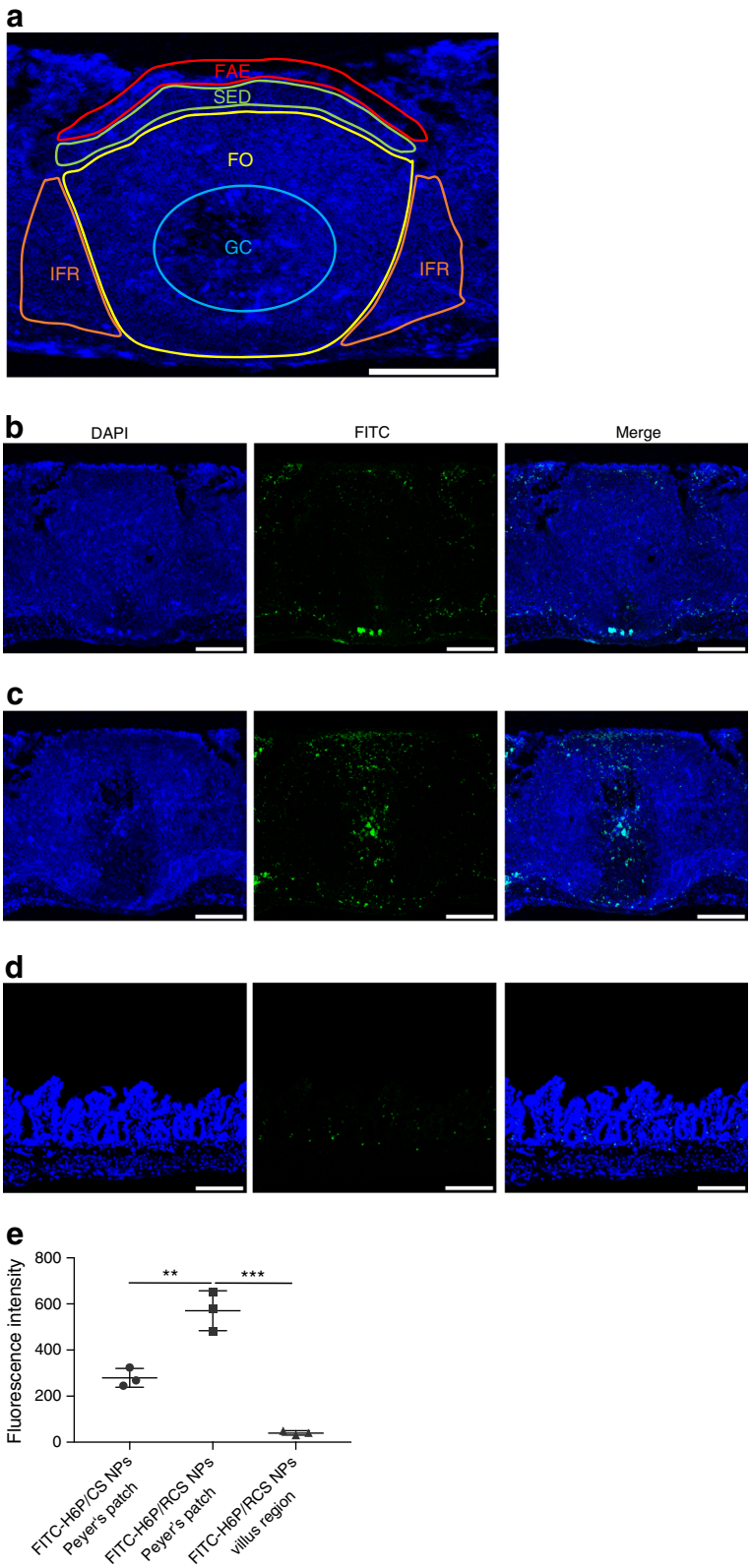

Fig. 4 (**a**) A CLSM image of a Peyer's patch, with the compartments outlined and labelled. FAE, follicle-associated epithelium; FO, follicle; GC, germinal centre; IFR, intrafollicular region; SED, subepithelial dome. (**b**,**c**) Localisation of FITC-H6P on a Peyer's patch at 1 h after injection of FITC-H6P/CS NPs (**b**) or FITC-H6P/RCS NPs (**c**) into the closed ileal loop. (**d**) Localisation of FITC-H6P on the villus region at 1 h after injection of FITC-H6P/RCS NPs into the closed ileal loop. FITC-H6P (green), DAPI staining (blue). Scale bars, 200 μm. (**e**) The fluorescence intensity of FITC in CLSM images was quantified using Image J2x software version 2.1.4.7 (Rawak Software, Stuttgart, Baden-Württemberg, Germany). The results of three independent experiments are displayed. Means and SDs are shown as lines. $^{**}p<0.01$, $^{***}p<0.001$

However, it should be noted that leukocytic infiltration was observed in some pancreatic islets in the H6P/RMCS NPs i. g. group (Fig. 6c,e), suggesting that the protective effects induced by H6P/RMCS NPs might weaken over time.

Oral vaccination with H6P/RMCS NPs activated an H6P-specific Th2-type humoral immune response Serum anti-H6P IgG antibody was measured to evaluate the antigen delivery efficiency of H6P/RMCS NPs. As shown in Fig. 7a, orally administered H6P/RMCS NPs produced high levels of anti-H6P IgG antibody, which were maintained for more than 12 weeks after the last immunisation. At 8 weeks of age, the serum anti-H6P IgG antibody level of mice treated with H6P/RMCS NPs was almost equivalent to that of mice treated with an s.c. injection of H6P solution, and was 4.8-fold higher than those treated with H6P i.g. The results suggest that H6P/RMCS NPs effectively deliver and release H6P in lymphoid tissues, inducing a high and continuous antigen-specific humoral immune response.

To identify the type of immune response, the serum isotype levels of IgG1 and IgG2a were determined. The IgG2a isotype is associated with a Th1-type response, while the IgG1 isotype is associated with a Th2-type response [31]. As shown in Fig. 7b, the anti-H6P antibodies in the H6P/RMCS NPs i.g. group and the H6P s.c. group were almost exclusively of the IgG1 subclass. The results suggest that vaccination with H6P activated an H6P-specific Th2-type response.

Spontaneous T cell proliferation in response to H6P was downregulated and the secretion of Th1-type cytokines was inhibited after H6P/RMCS NPs vaccination Splenocytes isolated from NOD mice were stimulated with H6P and concanavalin A (ConA), respectively. The proliferative responses of T cells to H6P and ConA were measured by analysing the CFSE dilution of gated $CD3^+$ cells. As shown in Fig. 8a, for the H6P/RMCS NPs i.g. group, the percentage of proliferated T cells was significantly lower than that of the RMCS NPs i.g. group ($p < 0.01$) after H6P stimulation. However, both groups showed similar proliferative responses to ConA (Fig. 8b), indicating that there was no general inhibition of T cell reactivity induced by H6P vaccination. The results indicate that the spontaneous T cell proliferative response to H6P in NOD mice was downregulated after H6P vaccination.

Splenocytes isolated from NOD mice were stimulated in vitro with H6P and the secreted cytokines were measured. As shown in Fig. 8c–f, splenocytes from mice treated with H6P/RMCS NPs i.g. produced higher levels of Th2-type cytokines (IL-4, IL-10) and lower levels of Th1-type cytokines (IFN-γ, IL-2) than those from mice treated with blank RMCS NPs i.g. (all $p < 0.01$). TGF-β plays a pivotal role in the

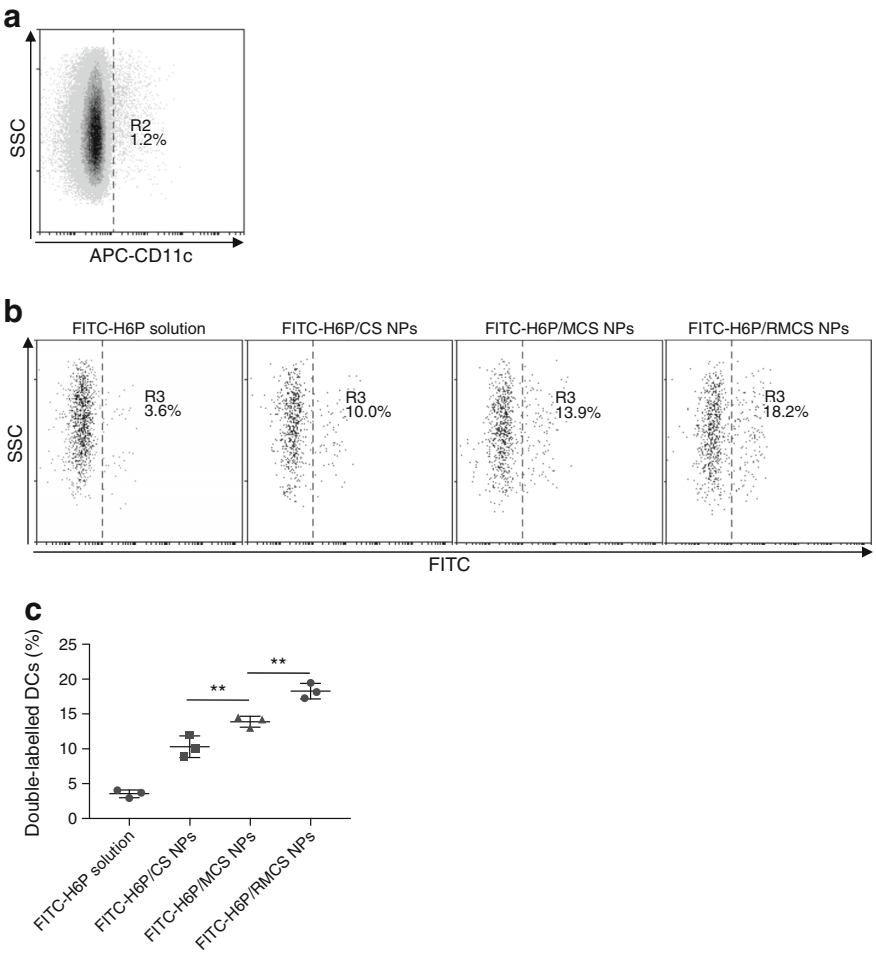

Fig. 5 FITC-H6P uptake by DCs in Peyer's patches after 1 h incubation with FITC-H6P solution, FITC-H6P-loaded CS NPs, MCS NPs and RMCS NPs. (**a**) $CD11c^+$ cells (R2) were gated based on allophycocyanin (APC) fluorescence. (**b**) FITC-H6P uptake in gated cells was analysed based on FITC fluorescence. SSC, side scatter. (**c**) The percentage FITC-H6P uptake by DCs in three independent experiments is presented. Means and SDs are shown as lines. $^{**}p<0.01$

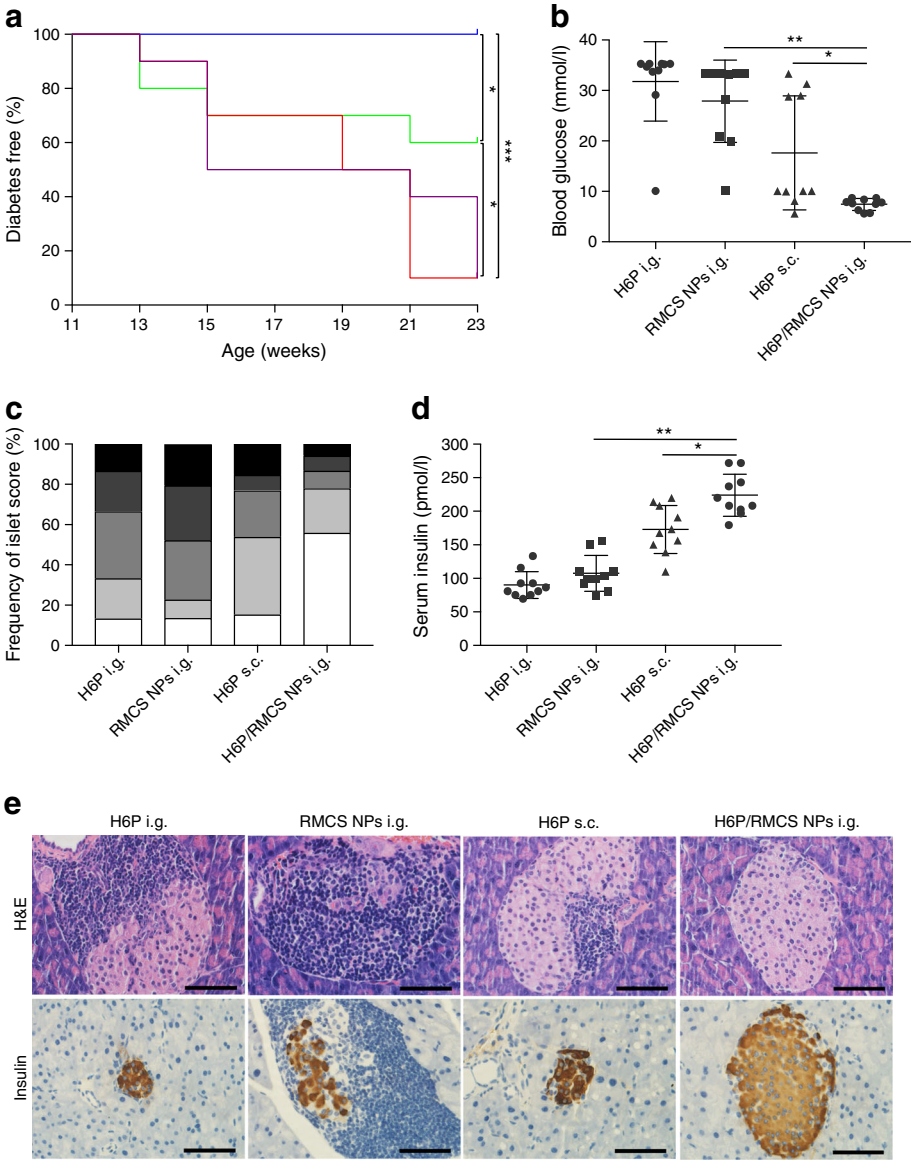

Fig. 6 Oral vaccination with H6P/RMCS NPs prevents autoimmune diabetes in NOD mice. (**a**) The frequency of diabetes-free mice over time. Purple line, H6P i.g.; red line, RMCS NPs i.g.; green line, H6P s.c.; blue line, H6P/RMCS NPs i.g. (n=10 mice per group). (**b**) Blood glucose of NOD mice at 23 weeks of age. Results from ten mice are displayed for each group; means and SDs are shown as lines. (**c**) Frequency of islets with various grades of insulitis. White, 0 (no infiltrate); light grey, 1 (0–25%); mid grey, 2 (25–50%); dark grey, 3 (50–75%); black, 4 (>75%). At least 50 islets were scored for each group. (**d**) Serum insulin levels of NOD mice at 23 weeks of age. Results from ten mice are displayed for each group; means and SDs are shown as lines. (**e**) Representative H&E staining and insulin immunohistochemical results from NOD mouse pancreas sections obtained at 23 weeks of age. Scale bars, 60 μm. *p<0.05, **p<0.01, ***p<0.001

induction of Tregs from naive T cells to treat autoimmune diseases [32, 33]. As shown in Fig. 8g, splenocytes from mice treated with H6P/RMCS NPs i.g. mice produced higher levels of TGF-β than those from mice treated with blank RMCS NPs

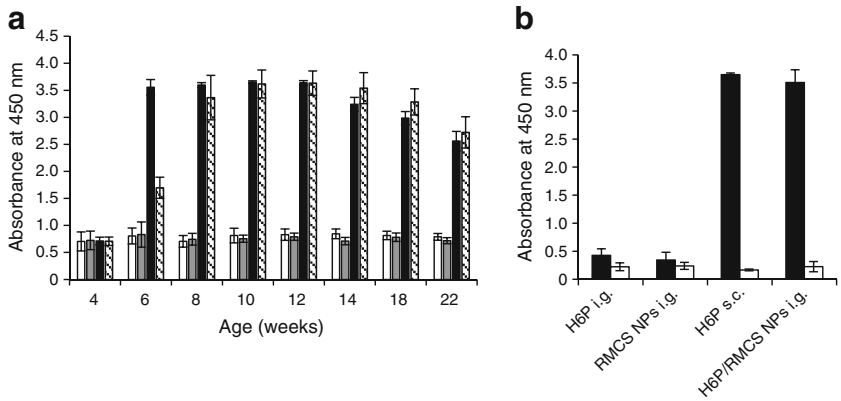

Fig. 7 (**a**) Serum anti-H6P IgG levels in NOD mice before (at 4 weeks of age) and after vaccination with H6P i.g. (white bars), RMCS NPs i.g. (grey bars), H6P s.c. (black bars) and H6P/RMCS NPs i.g. (striped bars). (**b**) Serum anti-H6P IgG1 (black bars) and IgG2a (white bars) levels in NOD mice at 12 weeks of age. The results are expressed as means ± SD of ten mice

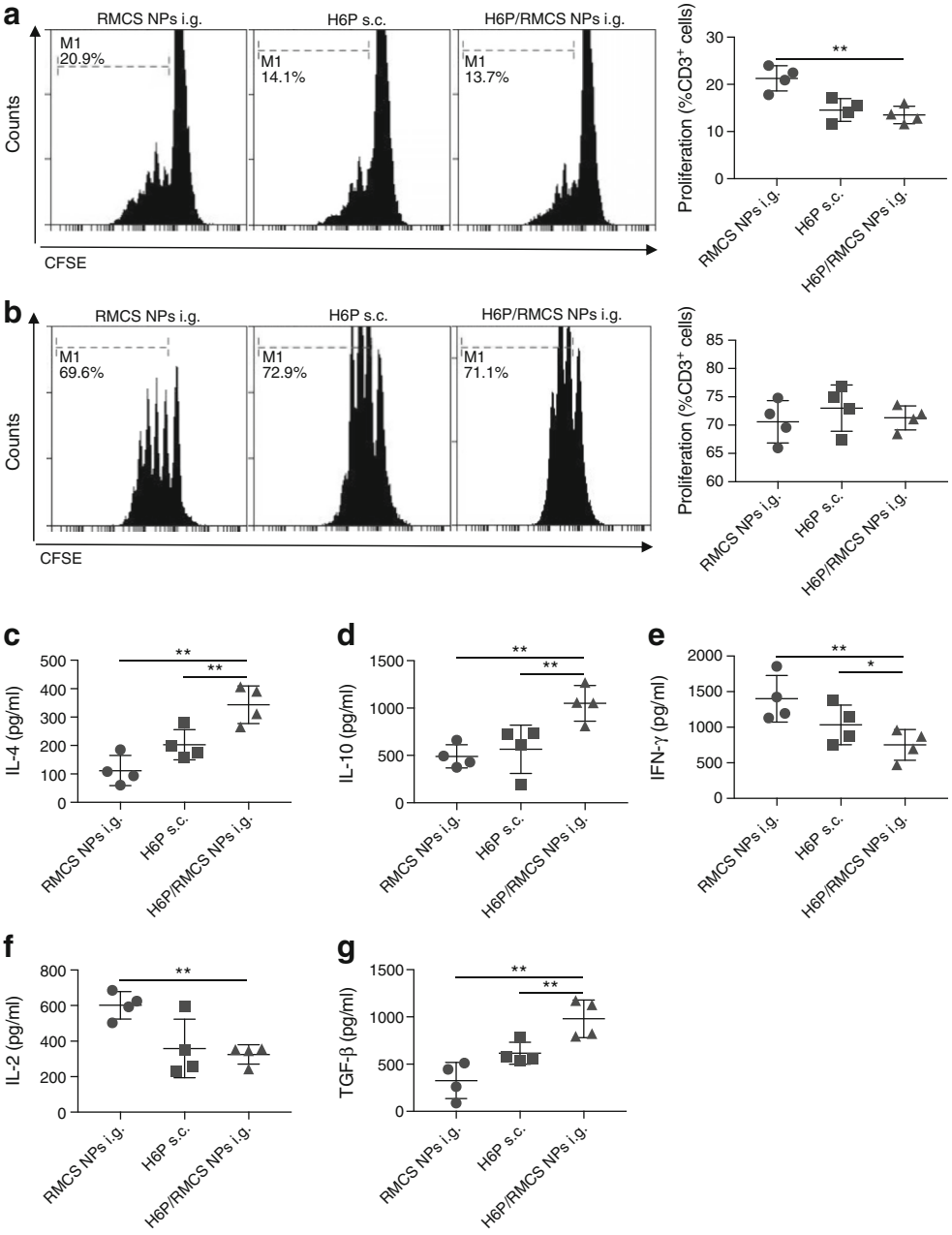

Fig. 8 Four weeks after vaccination with RMCS NPs i.g., H6P s.c. or H6P/RMCS NPs i.g., splenocytes were isolated from NOD mice for T cell proliferation and cytokine assay. (**a**,**b**) T cell proliferation following co-culture with H6P (**a**) or ConA (**b**) was analysed using a CFSE-based method. (**c**–**g**) Cytokine levels in the supernatant of spleen cells after H6P stimulation. Results from four mice are displayed for each group; means and SDs are shown as lines. *p<0.05, **p<0.01

i.g. ($p < 0.01$). These results suggest that the prevention of autoimmune diabetes is associated with the inhibition of Th1-type cytokine secretion and upregulation of Th2-type cytokines.

Oral vaccination with H6P/RMCS NPs increased the frequency of Tregs and decreased the frequency of Th1 cells Tregs play an important role in antigen-induced tolerance [34]. After vaccination of NOD mice with H6P/RMCS NPs i.g., the per cent of $CD4^+CD25^+FOXP3^+$ T cells was significantly increased ($p < 0.05$) in pancreatic draining lymph nodes (Fig. 9a), whereas the per cent of $CD4^+$T-bet^+ T cells was markedly decreased ($p < 0.01$) (Fig. 9b) compared with the blank RMCS NPs i.g. control.

Discussion

For type 1 diabetes immunotherapy, oral immunisation is an attractive route of vaccination. A number of preclinical studies have successfully prevented or treated autoimmune diabetes through the oral delivery of autoantigen [35–37]. However, the experimental animals in these studies needed to take a large dose of antigen for a long time

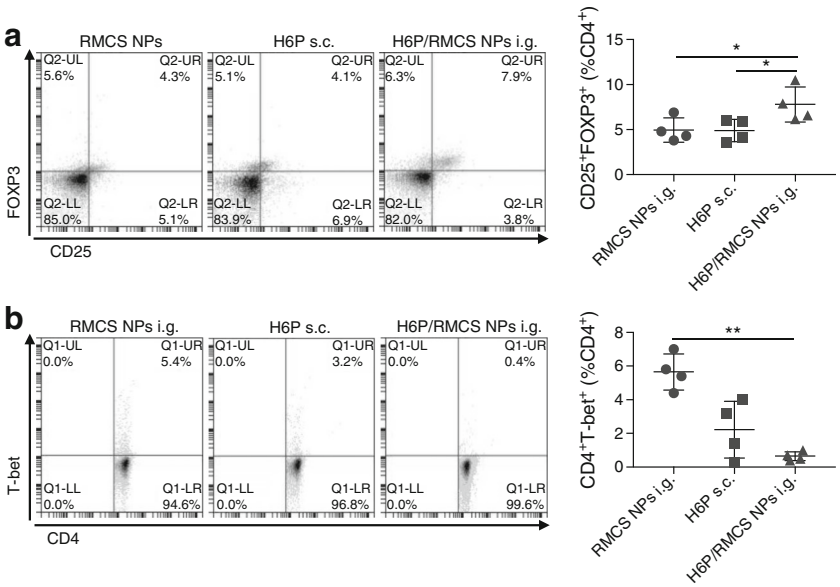

Fig. 9 (**a**,**b**) Four weeks after vaccination with RMCS NPs i.g., H6P s.c. or H6P/RMCS NPs i.g., $CD4^+CD25^+FOXP3^+$ T cells (**a**) and $CD4^+T\text{-}bet^+$ T cells (**b**) in the pancreatic draining lymph nodes of NOD mice were analysed by flow cytometry. Results from four mice are displayed for each group; means and SDs are shown as lines. $*p<0.05$, $**p<0.01$

and the therapeutic effect was limited. In NOD mice, oral administration of 1 mg insulin twice a week for 5 weeks and then weekly until 1 year of age has been reported to reduce the incidence of diabetes, but could not completely prevent the onset of diabetes [35]; in children genetically susceptible to type 1 diabetes, only a high oral dose of antigen (67.5 mg of insulin daily for 3–12 months) induced an immune response [38]. Therefore, we believe that low delivery efficiency of the antigen may be the main reason for the low efficiency of oral antigen therapy. In a previous study, genetically modified *Lactococcus lactis* that expressed H6P was used as a vector for intestinal delivery of H6P, but the recombinant *L. lactis* was administered for 36 weeks and 16.7–25% of NOD mice still developed diabetes [39]. In the current study, we observed that the onset of diabetes in NOD mice was 100% prevented through the oral administration of H6P/RMCS NPs once a week for 7 weeks. This ideal outcome may be attributed to the high antigen delivery efficiency of targeting H6P/RMCS NPs. The vaccination dose of H6P was chosen based on our previous study [6]. We chose to immunise the NOD mice from 4 to 10 weeks of age (i.e. once weekly for 7 weeks), before the onset of diabetes, because this was a prevention study and we thought that that multiple drug deliveries would be associated with a better outcome.

β1 integrins are overexpressed at the apical surface of human and mouse M cells. In addition, it has been demonstrated that grafting RGD peptide that targets β1 integrins onto NPs significantly increases their transport by M cells [21]. Mannose receptor is a 175 kDa transmembrane protein that is highly expressed on antigen-presenting cells such as DCs. It mediates the endocytosis, processing and presentation of antigens that expose mannose residues. Mannose-modified NPs have been widely used for DC-targeted delivery and show enhanced efficiency over other systems [22]. In this study, RGD and mannose were used to modify CS, and we observed that the in vivo uptake of H6P by DCs in Peyer's patches was enhanced significantly after its encapsulation in RMCS NPs. The characteristics of the DCs that take up the antigen (e.g. whether they are immature, activated or tolerogenic DCs) remain to be analysed in future studies. A further area of future study is identifying the distribution of the remaining antigen, whether in gut-associated lymphoid tissue or within the circulation.

Mechanisms of antigen-induced tolerance include deletion and/or anergy of effector T cells, immune deviation (Th1 to Th2) and induction of Tregs [40]. How these mechanisms are interrelated is not completely understood. Tregs and immune deviation could be outcomes of anergy; alternatively, Tregs could induce anergy in effector T cells. In this study, oral H6P/RMCS NPs increased the secretion of Th2-type cytokines and attenuated the secretion of Th1-type cytokines. These results are in line with those of a previous report, in which vaccination of NOD mice with H6P against autoimmune diabetes was associated with a Th1 to Th2 cytokine shift [6]. In addition, in the current study, oral H6P/RMCS NPs were associated with high levels of anti-H6P IgG1 antibody. This could be induced by HSP65 in the H6P antigen, which has about 50% homology with the human homologue HSP60 [41]. HSP60 can induce the proliferation of B cells [42]. The activated B cells have been reported to not only produce antibody, but also to inhibit spontaneous Th1 autoimmunity [43].

Whether the H6P/RMCS NPs vaccination promotes the generation of H6P-specific IgA in the gut lumen was not analysed in the current study. Because the H6P antigen is incorporated into NPs, we think that anti-H6P IgA is unlikely to interfere with the uptake of NPs upon repeated administration. In recent years, the central role of $CD4^+CD25^+FOXP3^+$ Tregs in maintaining peripheral immune tolerance has been confirmed [44]. Of clinical importance is the ability of Tregs to exert antigen-non-specific 'bystander' suppression. In addition, bystander suppression does not depend on the 'tolerising' autoantigen necessarily being the primary driver of pathology. Several studies have successfully prevented or treated diabetes in animal models by inducing antigen-specific Tregs [36, 45]. In this study, we observed that oral H6P/RMCS NPs increased the frequency of $CD4^+CD25^+FOXP3^+$ Tregs in pancreatic draining lymph nodes at 4 weeks after immunisation. However, whether these Tregs endure for a long time remains to be further studied. In addition, the characteristics of these Tregs (e.g. whether they are de novo induced or an expansion of pre-existing Tregs) is unclear. Of note, s.c. injection of H6P did not increase the frequency of Tregs. These results are in line with the theory that either systemic or mucosal administration of antigen can induce tolerance, but that the mucosal route appears more likely to induce Treg responses [40]. Overall, the mechanisms of action of oral H6P/RMCS NPs against autoimmune diabetes in NOD mice may involve immune deviation (Th1 to Th2) and induction of Tregs. More detailed studies need to be performed to further elucidate the mechanism of action of H6P/RMCS NPs, including T cell responses in the gut-associated lymphoid tissues, pancreatic draining lymph nodes and pancreas at different time points.

In this study, we demonstrated that H6P/RMCS NPs efficiently deliver H6P to DCs in Peyer's patches, induce antigen-specific T cell tolerance and prevent the onset of autoimmune diabetes in NOD mice. The results suggest that RMCS NPs are suitable for encapsulating biological macromolecules and may serve as a promising platform for oral delivery of autoantigens to induce tolerance.

Acknowledgements We thank Y. Xing (manager of flow cytometry at the China Pharmaceutical University) for her scientific advice and technical assistance with flow cytometry.

Data availability The datasets generated during and/or analysed during the current study are available from the corresponding author on reasonable request.

Funding This study was supported by National Natural Science Foundation of China (No. 30973650/H3008) and the Postgraduate Research & Practice Innovation Program of Jiangsu Province (KYCX17_0676).

Duality of interest The authors declare that there is no duality of interest associated with this manuscript.

Contribution statement YLC, JW, XJX and LZ contributed to the conception and design of the study. YLC, JJW, WJZ and BHX performed the experiments and analysed the results. YLC, JW, XJX and LZ drafted the manuscript. All authors revised the manuscript critically and gave final approval of the submitted version. LZ is the guarantor of the work.

References

1. van Belle TL, Coppieters KT, von Herrath MG (2011) Type 1 diabetes: etiology, immunology, and therapeutic strategies. Physiol Rev 91:79–118
2. Lernmark A, Larsson HE (2013) Immune therapy in type 1 diabetes mellitus. Nat Rev Endocrinol 9:92–103
3. Frumento D, Nasr MB, Essawy BE, D'Addio F, Zuccotti GV, Fiorina P (2017) Immunotherapy for type 1 diabetes. J Endocrinol Investig 40:803–814
4. Elias D, Reshef T, Birk OS, van der Zee R, Walker MD, Cohen IR (1991) Vaccination against autoimmune mouse diabetes with a T cell epitope of the human 65-kDa heat shock protein. Proc Natl Acad Sci U S A 88:3088–3091
5. Abulafia-Lapid R, Elias D, Raz I, Keren-Zur Y, Atlan H, Cohen IR (1999) T cell proliferative responses of type 1 diabetes patients and healthy individuals to human hsp60 and its peptides. J Autoimmun 12:121–129
6. Jin L, Zhu A, Wang Y et al (2008) A Th1-recognized peptide P277, when tandemly repeated, enhances a Th2 immune response toward effective vaccines against autoimmune diabetes in nonobese diabetic mice. J Immunol 180:58–63
7. Xu D, Prasad S, Miller SD (2013) Inducing immune tolerance: a focus on type 1 diabetes mellitus. Diabetes Manag 3:415–426
8. Li AF, Escher A (2003) Intradermal or oral delivery of GAD-encoding genetic vaccines suppresses type 1 diabetes. DNA Cell Biol 22:227–232
9. Mowat AM (2003) Anatomical basis of tolerance and immunity to intestinal antigens. Nat Rev Immunol 3:331–341
10. Matzinger P, Kamala T (2011) Tissue-based class control: the other side of tolerance. Nat Rev Immunol 11:221–230
11. Rimoldi M, Chieppa M, Salucci V et al (2005) Intestinal immune homeostasis is regulated by the crosstalk between epithelial cells and dendritic cells. Nat Immunol 6:507–514
12. Mucida D, Park Y, Kim G et al (2007) Reciprocal TH17 and regulatory T cell differentiation mediated by retinoic acid. Science 317:256–260
13. Banchereau J, Briere F, Caux C et al (1999) Immunobiology of dendritic cells. Annu Rev Immunol 18:767–811
14. Everson MP, Lemak DG, McDuffie DS, Koopman WJ, McGhee JR, Beagley KW (1998) Dendritic cells from Peyer's patch and spleen induce different T helper cell responses. J Interf Cytokine Res 18:103–115
15. Hashiguchi M, Hachimura S, Ametani A et al (2011) Naïve CD4+ T cells of Peyer's patches produce more IL-6 than those of spleen in response to antigenic stimulation. Immunol Lett 141:109–115
16. Iwasaki A, Kelsall BL (1999) Freshly isolated Peyer's patch, but not spleen, dendritic cells produce interleukin 10 and induce the differentiation of T helper type 2 cells. J Exp Med 190:229–239
17. Peron JP, de Oliveira AP, Rizzo LV (2009) It takes guts for tolerance: the phenomenon of oral tolerance and the regulation of autoimmune response. Autoimmun Rev 9:1–4
18. Wang X, Sherman A, Liao G et al (2013) Mechanism of oral tolerance induction to therapeutic proteins. Adv Drug Deliv Rev 65:759–773

19. Kraehenbuhl JP, Neutra MR (2000) Epithelial M cells: differentiation and function. Annu Rev Cell Dev Biol 16:301–332
20. Davitt CJ, Lavelle EC (2015) Delivery strategies to enhance oral vaccination against enteric infections. Adv Drug Deliv Rev 91:52–69
21. Garinot M, Fiévez V, Pourcelle V et al (2007) PEGylated PLGA-based nanoparticles targeting M cells for oral vaccination. J Control Release 120:195–204
22. Raviv L, Jaron-Mendelson M, David A (2015) Mannosylated polyion complexes for in vivo gene delivery into CD11c^{+} dendritic cells. Mol Pharm 12:453–462
23. Yao W, Jiao Y, Luo J, Du M, Zong L (2012) Practical synthesis and characterization of mannose-modified chitosan. Int J Biol Macromol 50:821–825
24. Wang C, Chen B, Zou M, Cheng G (2014) Cyclic RGD-modified chitosan/graphene oxide polymers for drug delivery and cellular imaging. Colloids Surf B Biointerfaces 122:332–340
25. Biswas S, Chattopadhyay M, Sen KK, Saha MK (2015) Development and characterization of alginate coated low molecular weight chitosan nanoparticles as new carriers for oral vaccine delivery in mice. Carbohydr Polym 121:403–410
26. Primard C, Rochereau N, Luciani E et al (2010) Traffic of poly (lactic acid) nanoparticulate vaccine vehicle from intestinal mucus to sub-epithelial immune competent cells. Biomaterials 31:6060–6068
27. Mariño E, Richards JL, McLeod KH et al (2017) Gut microbial metabolites limit the frequency of autoimmune T cells and protect against type 1 diabetes. Nat Immunol 18:552–562
28. Qi F, Wu J, Yang T, Ma G, Su Z (2014) Mechanistic studies for monodisperse exenatide-loaded PLGA microspheres prepared by different methods based on SPG membrane emulsification. Acta Biomater 10:4247–4256
29. Lai J, Shah BP, Garfunkel E, Lee KB (2013) Versatile fluorescence resonance energy transfer-based mesoporous silica nanoparticles for real-time monitoring of drug release. ACS Nano 7:2741–2750
30. Jiang PL, Lin HJ, Wang HW et al (2015) Galactosylated liposome as a dendritic cell-targeted mucosal vaccine for inducing protective anti-tumor immunity. Acta Biomater 11:356–367
31. Maassen CB, Boersma WJ, Van Holten-Neelen C, Claassen E, Laman JD (2003) Growth phase of orally administered *Lactobacillus* strains differentially affects IgG1/IgG2a ratio for soluble antigens: implications for vaccine development. Vaccine 21:2751–2757
32. Bilate AM, Lafaille JJ (2012) Induced CD4^{+}Foxp3^{+} regulatory T cells in immune tolerance. Annu Rev Immunol 30:733–758
33. Fei L, Wang L, Jin XM, Yan CH, Shan J, Shen XM (2009) The immunologic effect of TGF-beta1 chitosan nanoparticle plasmids on ovalbumin-induced allergic BALB/c mice. Immunobiology 214:87–99
34. Sakaguchi S (2000) Regulatory T cells: key controllers of immunologic self-tolerance. Cell 101:455–458
35. Zhang ZJ, Davidson L, Eisenbarth G, Weiner HL (1991) Suppression of diabetes in nonobese diabetic mice by oral administration of porcine insulin. J Endocrinol Investig 88:10252–10256
36. Bergerot I, Arreaza GA, Cameron MJ et al (1999) Insulin B-chain reactive CD4^{+} regulatory T cells induced by oral insulin treatment protect from type 1 diabetes by blocking the cytokine secretion and pancreatic infiltration of diabetogenic effector T cells. Diabetes 48:1720–1729
37. Takiishi T, Korf H, Van Belle TL et al (2012) Reversal of autoimmune diabetes by restoration of antigen-specific tolerance using genetically modified *Lactococcus lactis* in mice. J Clin Invest 122:1717–1725
38. Bonifacio E, Ziegler AG, Klingensmith G et al (2015) Effects of high-dose oral insulin on immune responses in children at high risk for type 1 diabetes: the Pre-POINT randomized clinical trial. JAMA 313:1541–1549
39. Ma Y, Liu J, Hou J et al (2014) Oral administration of recombinant *Lactococcus lactis* expressing HSP65 and tandemly repeated P277 reduces the incidence of type I diabetes in non-obese diabetic mice. PLoS One 9:e105701
40. Harrison LC, Hafler DA (2000) Antigen-specific therapy for autoimmune disease. Curr Opin Immunol 12:704–711
41. Jindal S, Dudani AK, Singh B, Harley CB, Gupta RS (1989) Primary structure of a human mitochondrial protein homologous to the bacterial and plant chaperonins and to the 65-kilodalton mycobacterial antigen. Mol Cell Biol 9:2279–2283
42. Cohensfady M, Nussbaum G, Pevsnerfischer M et al (2005) Heat shock protein 60 activates B cells via the TLR4-MyD88 pathway. J Immunol 175:3594–3602
43. Tian J, Zekzer D, Hanssen L, Lu Y, Olcott A, Kaufman DL (2001) Lipopolysaccharide-activated B cells down-regulate Th1 immunity and prevent autoimmune diabetes in nonobese diabetic mice. J Immunol 167:1081–1089
44. Wing K, Sakaguchi S (2010) Regulatory T cells exert checks and balances on self tolerance and autoimmunity. Nat Immunol 11:7–13
45. Kasagi S, Zhang P, Che L et al (2014) In vivo-generated antigen-specific regulatory T cells treat autoimmunity without compromising antibacterial immune response. Sci Transl Med 6:241–278